The Journal of Chemical Physics

RESEARCH ARTICLE | APRIL 09 2024

Analysis on high-resolution spectrum of the S_1–S_0 transition of free-base phthalocyanine

Yuki Miyamoto ; Ayami Hiramoto ; Kana Iwakuni ; Susumu Kuma ; Katsunari Enomoto ; Naofumi Nakayama ; Masaaki Baba

J. Chem. Phys. 160, 144304 (2024)
https://doi.org/10.1063/5.0191810

AIP Publishing

The Journal of Chemical Physics ARTICLE pubs.aip.org/aip/jcp

Analysis on high-resolution spectrum of the S_1–S_0 transition of free-base phthalocyanine

Cite as: J. Chem. Phys. 160, 144304 (2024); doi: 10.1063/5.0191810
Submitted: 16 December 2023 • Accepted: 21 March 2024 •
Published Online: 9 April 2024

Yuki Miyamoto,[1,a] Ayami Hiramoto,[1] Kana Iwakuni,[2] Susumu Kuma,[3] Katsunari Enomoto,[4] Naofumi Nakayama,[5] and Masaaki Baba[6,7]

AFFILIATIONS

[1] Research Institute for Interdisciplinary Science, Okayama University, Kita-ku, Okayama 700-8530, Japan
[2] Institute for Laser Science, University of Electro-Communications, Chofu, Tokyo 182-8585, Japan
[3] Atomic, Molecular and Optical Physics Laboratory, RIKEN, Wako, Saitama 351-0198, Japan
[4] Department of Physics, University of Toyama, Toyama 930-8555, Japan
[5] CONFLEX Corporation, 3-23-17 Takanawa, Minato-ku, Tokyo 108-0074, Japan
[6] Molecular Photoscience Research Center, Kobe University, Kobe 657-8501, Japan
[7] Division of Chemistry, Graduate School of Science, Kyoto University, Kyoto 606-8502, Japan

[a] **Author to whom correspondence should be addressed:** miyamo-y@okayama-u.ac.jp

ABSTRACT

A high-resolution absorption spectrum of the S_1–S_0 transition of free-base phthalocyanine was observed and analyzed with improved reliability. The spectrum, with a partially resolved rotational structure, was obtained by using the buffer-gas cooling technique and a single-mode tunable laser. Our new analysis reveals that the $S_1 \leftarrow S_0$ 0_0^0 band belongs to the *a*-type transition, where the electronic transition moment aligns parallel to the NH–HN direction, allowing the assignment of the S_1 state to $^1B_{3u}$. These results agree with a prior study using supersonic expansion and are well supported by theoretical calculations. Interestingly, the rotational constant B in the S_1 state, which is often smaller than that in the ground state for typical molecules, was found to be slightly larger than that in the S_0 ^1A_g state. This suggests a change in the character of π bonds with the electronic excitation.

INTRODUCTION

Recent advancements in electron microscopy[1] and scanning probe microscopy[2] enable precise determination of structures of large molecules with an unprecedented spatial resolution. However, understanding the structures of these molecules and their quantum properties remains challenging, particularly in the gas phase. Consequently, the spectroscopic study of these molecules in the gas phase at the rotationally resolved precision is essential because the high-resolution spectra contain rich and detailed information. The combination of buffer-gas cooling technique with narrow bandwidth lasers has proven to be a powerful tool for high-resolution spectroscopy.[3–22] We have developed a measurement system that allows for the observation of a high-resolution electronic spectrum using a single-mode tunable ring dye laser.

Free-base phthalocyanine (FBPc, $C_{32}H_{18}N_8$) holds a pivotal role in pigment chemistry, being vital for various applications such as organic semiconductors, organic electro-luminescence displays, and phototherapy. Despite numerous spectroscopic studies,[23–33] a comprehensive examination and discussion regarding its molecular geometric structure and electronic excited states are necessary for optimizing the utilization of this molecule. Recently, Schlaghaufer and Slenczka have reported a high-resolution fluorescence excitation spectrum of FBPc with partially resolved rotational structures in a supersonic jet.[32] The authors presented a computational method to analyze the spectrum and derived the rotational constants. They concluded that the $S_1 \leftarrow S_0$ transition is predominantly *a*-type and assigned the S_1 state to the $^1B_{3u}$ state. Later, we reported a high-resolution absorption spectrum of buffer-gas-cooled FBPc.[33] However, our initial analysis does not align with their findings. This

disparity highlights the challenges in analyzing the spectra with partially resolved rotational structures. Obtaining an accurate spectrum and incorporating quantum chemical calculations for molecular structure and energies are essential for a more reliable analysis. While the analysis of experimental results yields solely spectroscopic constants, we can estimate the molecular structure through quantum chemical calculations that align with these experimental constants.

In a previous paper,[33] we roughly reproduced the overall spectrum shape by simulation. In this paper, we present a newly obtained spectrum with high stability and its analysis with improved reliability, accompanied with a theoretical calculation using density functional theory (DFT) and high-level *ab initio* methods. Our present analysis yields results that are fundamentally consistent with those of Ref. 32. We delve into the molecular geometry and electronic excited states of the isolated FBPc molecule based on theoretical calculations, discussing the resulting rotational constants and inertial defects.

EXPERIMENTAL

Figure 1(a) depicts the chemical structure diagram of FBPc. In this paper, we designate the *x*-axis as the *a*-axis and the *y*-axis as the *b*-axis. The apparatus is schematically illustrated in Fig. 1(b), resembling the setup already presented in our prior reports.[19,33] Commercially obtained free-base phthalocyanine (FBPc) from Tokyo Chemical Industry, with a purity exceeding 93%, was utilized without further purification. The powder sample was compressed at 70 MPa to form a solid pellet. This pellet was placed in a buffer gas cell, cooled to ~5 K during the experiment using a pulse tube cryocooler. FBPc vapor was produced by laser ablation (pulsed Nd:YAG laser, wavelength 532 nm, width ~10 ns) inside the cell and subsequently cooled through collisions with the helium buffer-gas atoms.

A single-mode ring dye laser (Coherent, 699-21, wavelength 661 nm, linewidth ~0.0001 cm^{-1}, dye: DCM), pumped by a diode laser (Civil Laser, wavelength 455 nm), was introduced into the cell to measure the absorption spectra. The power of the laser light transmitted through the cell was measured using a silicon photodetector. The laser power fluctuation was monitored before entering the chamber by sampling a small portion of the laser beam (not shown in the figure) and was used to derive the absorbance. In addition, we monitored the absorbance at a specific wavelength (15 131.7 cm^{-1}) using a diode laser (Thorlabs, HL6545MG). This absorbance corresponds to the amount of vaporized FBPc molecules due to ablation. The instability in the amount of vaporized molecules had previously caused fluctuations in the spectra. Normalizing the absorption signal by the amount of vaporized FBPc significantly improved the reliability and repeatability of the measurements. The wavenumber of the lasers was measured using a wavemeter (Highfinesse, WS-6) and calibrated by measuring a Doppler-free saturation spectrum of iodine molecules.[34] The uncertainty of the wavenumber was approximately estimated to be 0.0003 cm^{-1}.

RESULTS AND DISCUSSION

The $S_1 \leftarrow S_0$ 0_0^0 band of buffer-gas-cooled FBPc is observed around 15 132 cm^{-1}. The observed high-resolution spectrum is illustrated in Fig. 2. The red line represents the observed spectrum, while the blue line represents the simulated spectrum discussed below. The black line is the simulated spectrum using the rotational constants reported in Ref. 32. These spectra exhibit good agreement, especially around the center. Based on the simulation, the rotational temperature is estimated to be around 6 K, and the Doppler width of each rotational line is 0.0016 cm^{-1}, corresponding to a translational temperature of 10 K. The gentle structure around the band center with a dip was assigned to the Q transitions ($\Delta J = 0$), and the regular peak series on both sides were assigned to the P and R transitions

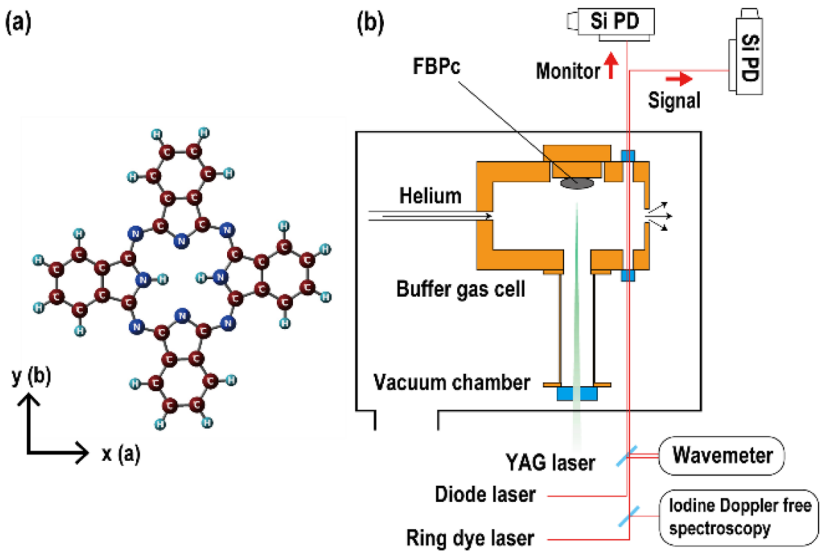

FIG. 1. (a) Chemical structure of FBPc. (b) Experimental apparatus.

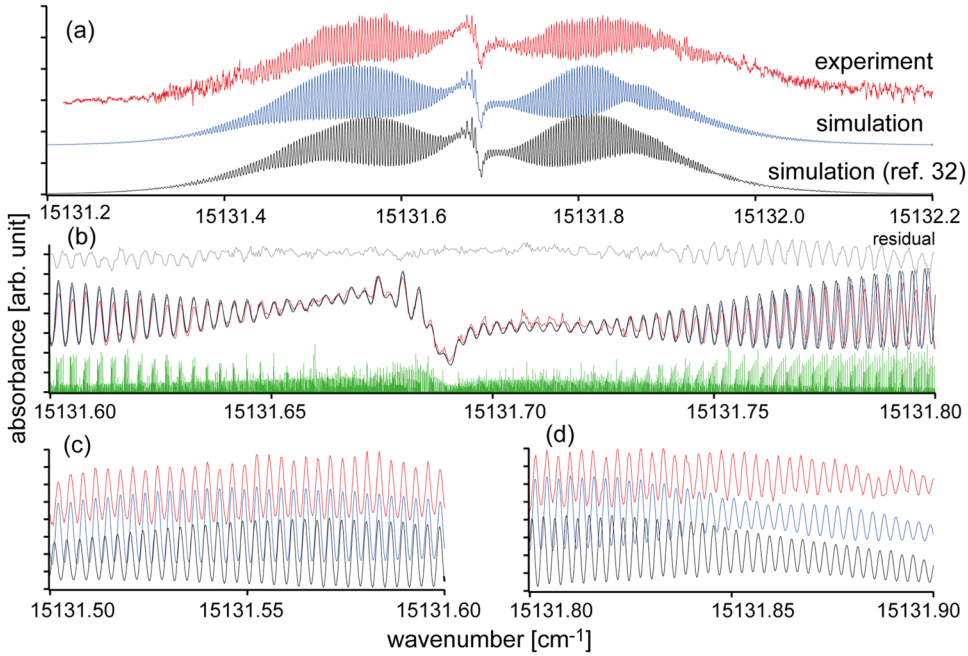

FIG. 2. (a) Observed (red) and simulated (blue, black) spectra of the $S_1 \leftarrow S_0$ transition of FBPc. (b)–(d) Enlarged spectra. For clarity, arbitrary offsets have been applied to the spectra. A gray trace in (b) shows the difference between the experiment (red) and simulation (blue). The stick spectrum (green) at the bottom in (b) depicts individual rotational lines as per our simulation.

($\Delta J = \pm 1$). Each peak is composed of many rotational lines [Fig. 2(b)]. We found that the rotational constants in Ref. 32 can reproduce the spectrum very well around the center. However, there are deviations on the order of 10 MHz in the outer regions [Figs. 2(c) and 2(d)]. Although this potentially arises from a miscalibration of the laser frequency, we attempted an alternative analysis of our spectrum. The current spectrum exhibits slight variations compared to that of Ref. 32. This discrepancy is notable especially in the central region of the spectrum, where the shape deviates from that of Ref. 32. In addition, the contrast of the oscillatory pattern is more pronounced in the current spectrum compared to the reference. These distinctions can be ascribed to differences in the rotational distribution.

The FBPc molecule has been conventionally regarded as planar (D_{2h}) in its ground state (S_0), as supported by earlier spectroscopic and theoretical studies. We conducted *ab initio* theoretical calculations for geometry optimization using various methods by the Gaussian16 program package,[35] assuming the D_{2h} symmetry. Subsequently, we performed spectral analysis using the PGOPHER program,[36] utilizing the calculated rotational constants as initial parameters. We employed the A-reduced Hamiltonian method designed for asymmetric-top molecules, as presented by Watson.[37] We fine-tuned the rotational constants manually to replicate the observed spectrum accurately. Through a series of trial-and-error fitting procedures, we achieved a spectral contour that closely matched the observed one, assuming an *a*-type band, consistent with the findings of Ref. 32. We attempted a more precise reproduction of the spectral contour using the contour fitting function of PGOPHER. The optimal-fit rotational constants are tabulated in Table I.

It is essential to note that the observed spectrum could not be accurately reproduced using solely the rigid-rotor rotational constants (A, B, and C). Second-order terms were necessary to achieve a good correspondence. Δ_J, Δ_{JK}, and Δ_K are quartic centrifugal distortion constants for symmetric-top molecules, while δ_J and δ_K represent asymmetric-top distortion constants. The A, B, and C values were obtained by fitting the central portion of the spectrum (15 131.60–15 131.75 cm^{-1}) using fixed higher-order terms. Subsequently, the higher-order terms were determined by fitting a wider range profile (15 131.4–15 132.0 cm^{-1}) while keeping the rigid-rotor terms constant. This iterative process was carried out to derive the result. The selection of these regions is arbitrary and influences the results. This also suggests that the criteria for a good fit carry a degree of arbitrariness. While this arbitrariness complicates a strictly quantitative discussion, we maintain that the fundamental conclusion remains unchanged. By including higher-order terms, we achieved a better reproduction of the spectrum's outer regions while maintaining good agreement at the center. The obtained rotational constants are mostly in agreement between the two experiments (Table I), although minor discrepancies exist. The consistency of the rotational constants derived from slightly different spectra lends credibility to both analyses. Notably, T_0 exhibits a relatively large deviation of 0.0009 cm^{-1}, exceeding our uncertainty of 0.0003 cm^{-1}. There is a slight deviation in peak positions at higher wavenumber regions above 15 131.85 cm^{-1}. This discrepancy may be attributed to experimental factors or higher-order effects.

TABLE I. Summary of spectroscopic constants of the S_0 and S_1 states of FBPc. A, B, and C are rigid-rotor rotational constants. Δ_J, Δ_{JK}, and Δ_K are quartic centrifugal distortion constants for symmetric-top molecules, while δ_J and δ_K represent asymmetric-top distortion constants. T_0 is a band origin. Δ is the inertial defect. Single (double) primes show constants for the S_1 (S_0) state. The unit for all values is cm^{-1}, except for inertial defects. Numbers in parentheses represent fitting errors provided by PGOPHER or errors given by Ref. 32.

	Experiment	Calculation	Reference 32
A'' ($\times 10^{-3}$)	2.9899 (40)	2.9900	2.9903 (12)
B'' ($\times 10^{-3}$)	2.9760 (13)	2.9831	2.9758 (10)
C'' ($\times 10^{-3}$)	1.4916 (24)	1.4933	1.4930 (2)
Δ_K'' ($\times 10^{-10}$)	1.44 (3)		
Δ_{JK}'' ($\times 10^{-10}$)	1.80 (5)		
Δ_J'' ($\times 10^{-10}$)	−23.2 (3)		
δ_K'' ($\times 10^{-10}$)	5.06 (10)		
δ_J'' ($\times 10^{-10}$)	0.50 (1)		
Δ'' (amu Å^2)	−1.1	−0.2	−11
T_0	15 131.6882	16 243	15 131.6891
A' ($\times 10^{-3}$)	2.9804 (31)	2.9859	2.9805 (11)
B' ($\times 10^{-3}$)	2.9783 (22)	2.9848	2.9783 (10)
C' ($\times 10^{-3}$)	1.4901 (24)	1.4927	1.4911 (2)
Δ_K' ($\times 10^{-10}$)	1.60 (3)		
Δ_{JK}' ($\times 10^{-10}$)	2.20 (5)		
Δ_J' ($\times 10^{-10}$)	−24.6 (3)		
δ_K' ($\times 10^{-10}$)	5.20 (10)		
δ_J' ($\times 10^{-10}$)	0.57 (1)		
Δ' (amu Å^2)	−3.2	−0.19	−11

The previous SAC-CI calculations have predicted that there are two closely situated low-lying excited states, $^1B_{2u}$ and $^1B_{3u}$, which are linked to the ground S_0 ^1A_g state through allowed $\pi\pi^*$ transitions.[38,39] These states are potential candidates for the observed S_1 state. According to molecular symmetry, the $^1B_{2u}$ ($^1B_{3u}$) state can be excited via a $b(a)$-type transition from the S_0 state. Because the $S_1 \leftarrow S_0$ 0_0^0 band is of a-type, we concluded that the S_1 state is assigned to the $^1B_{3u}$ state. As mentioned earlier, this aligns with the conclusions drawn in Ref. 32. This result is consistent not only with the previous SAC-CI calculation but also with our own calculations.

It is valuable to compare the experimentally obtained rotational constants with the results of theoretical calculations. Because the dispersion correction of the functionals is crucial for accurate calculation in DFT,[40,41] we employed ωB97XD, APFD, and MN15 for the functionals and 6-31G(d) and 6-311+G(2d,p) for the basis set. ωB97XD[40] and APFD[41] are functionals that incorporate recently developed dispersion corrections. MN15,[42] although lacking dispersion correction, has been optimized using a large database and shows good results even in systems dominated by dispersion. As a result, the calculation using the MN15 functional and 6-31G(d) basis set [MN15/6-31G(d)] provided rotational constants closest to our best-fit values for both S_0 and S_1 states (Table I).

Although the fundamental reason for the best match with MN15/6-31G(d) is not clear, it is plausible to infer that differences arise from the unique characteristics on the dispersion correction. The fact that rotational constants align with high accuracy for both

TABLE II. Results of SAC-CI/6-31G(d)//MN15/6-31G(d) calculation.

State	Main configuration ($\lvert d\rvert > 0.2$)	EE[a]	Osc[b]
$^1B_{3u}$	−0.93 ($4a_u \rightarrow 6b_{3g}$) +0.20 ($7b_{1u} \rightarrow 6b_{2g}$)	15 426	0.679
$^1B_{2u}$	0.95 ($4a_u \rightarrow 6b_{2g}$)	16 191	0.719

[a]Excitation energy in cm^{-1}.
[b]Oscillator strength.

S_0 and S_1 suggests that the calculation is robust enough to discuss the structures of the molecule. Although the rotational constants of S_0 and S_1 states are well reproduced by DFT and time-dependent (TD-)DFT calculations, the $S_1 \leftarrow S_0$ transition energy (T_0) is overestimated to the observed ones. Table II shows the results of SAC-CI calculations for the S_1 $^1B_{3u}$ and S_2 $^1B_{2u}$ states with MN15/6-31G(d) optimized geometry. The excitation energy of the S_1 $^1B_{3u}$ state is close to the observed values. The S_1 (S_2) state predominantly consists of the $4a_u \rightarrow 6b_{3g}$ ($4a_u \rightarrow 6b_{2g}$) configuration. Figure 3 depicts the calculated occupied and unoccupied molecular orbitals at HF/6-31G(d)//MN15/6-31G(d). The first and second HOMOs are a_u and b_{1u}, and the first and second LUMOs are b_{2g} and b_{3g}. The calculation exhibits separated HOMOs and nearly degenerate LUMOs. These results agree with the previous SAC-CI calculation.[38,39] A more quantitative discussion of the calculations will be presented in a separate paper.

Here, we discuss the molecular structure in the electronically excited state S_1 of FBPc. It is generally expected that the π bond is slightly lengthened by $\pi\pi^*$ electronic excitation due to an increase in the anti-bonding character in the π^* orbital. This usually results in smaller rotational constants in the excited state. However, our analysis of the experimental results reveals that the rotational constant B in the S_1 state is slightly larger than that in the S_0 state. We

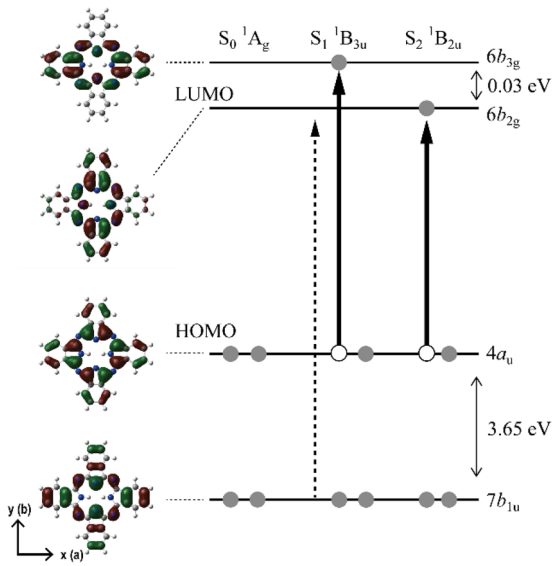

FIG. 3. Occupied and unoccupied molecular orbitals at HF/6-31G(d)//MN15/6-31G(d).

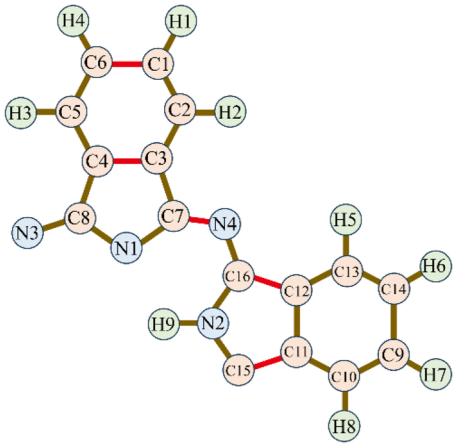

FIG. 4. Numbering of atoms in the FBPc molecule.

found that this bond shortening in the S_1 state can be explained by the spatial distribution of the π and π* orbitals (Fig. 3). The S_1 state is mainly represented by electronic excitation from $4a_u$ to $6b_{3g}$. The $6b_{3g}$ molecular orbital exhibits a strong π bonding character in the N4–C7, C12–C16, and C11–C15 bonds, while the C1–C6 and C3–C4 bonds have a node in $4a_u$. These bonds are indicated by red lines in Fig. 4. Table III presents the results of theoretical calculations with geometry optimization for the bond lengths in the S_0 and S_1 states. The bonds N4–C7, C1–C6, C3–C4, and C12–C16 and their equivalent bonds are shorter in the S_1 state (C11–C15 is equivalent to C12–C16). These bonds are along the $x(a)$ axis, causing the rotational constant B to increase due to the ππ* excitation. Our calculated A and B values exhibit consistent trends. The larger rotational constants in the excited states are observed in some polycyclic aromatic hydrocarbons (PAHs) of D_{2h} symmetry, such as tetracene[43] and anthracene.[44]

TABLE III. Calculated equilibrium bond lengths in the S_0 ^1A_g and S_1 $^1B_{3u}$ states of FBPc by MN15/6-31G(d) and TD-MN15/6-31G(d) calculations in the units of nanometer.

Bond	S_0 ^1A_g	S_1 $^1B_{3u}$	S_1–S_0
N1–C7	0.1361	0.1367	0.0007
N4–C7	0.1335	0.1330	−0.0005
N4–C16	0.1317	0.1330	0.0013
N2–C16	0.1375	0.1377	0.0002
C1–C2	0.1395	0.1401	0.0006
C1–C6	0.1406	0.1401	−0.0005
C2–C3	0.1392	0.1388	−0.0004
C3–C4	0.1399	0.1397	−0.0002
C3–C7	0.1465	0.1470	0.0005
C9–C14	0.1411	0.1413	0.0002
C11–C12	0.1407	0.1414	0.0007
C12–C13	0.1397	0.1399	0.0001
C12–C16	0.1451	0.1442	−0.0009
C13–C14	0.1389	0.1399	0.0010

We should also validate the rotational constants by considering the inertial defect, which is zero for rigid planar molecules and a small positive value for small planar molecules due to vibration–rotation interactions. Both Ref. 32 and our analysis suggested the small negative values in the S_0 and S_1 states even with significant uncertainties. As already discussed in Ref. 32, the occurrence of a negative inertial defect is common in many planar molecules and has been attributed to low-frequency out-of-plane vibrations. Oka derived empirical formulas for the inertial defect for aliphatic (Δ_{ali}) and aromatic (Δ_{aro}) molecules as follows:[45]

$$\Delta_{ali} = -\frac{33.715}{\nu} + 0.0186\sqrt{I_c},$$

$$\Delta_{aro} = -\frac{33.715}{\nu} + 0.008\ 03\sqrt{I_c},$$

where ν is the energy of the lowest out-of-plane vibration in cm^{-1}. The units of Δ and I_c are amu Å^2. In the case of the large molecules, there are many low-frequency out-of-plane vibrations. Assuming the contribution of each low-frequency mode to be additive, we can make an approximate estimate of the inertial defect. Menapace and Bernstein reported nine low-frequency out-of-plane modes of FBPc from 16 to 102 cm^{-1}.[27] Our estimated value of $C'' = 0.001\ 49\ cm^{-1}$ implies $I_c = 1.1 \times 10^4$ amu Å^2 in the S_0 states. The estimated inertial defect is $\Delta_{ali} = -5.5$ amu Å^2 and $\Delta_{aro} = -6.6$ amu Å^2. These negative values substantiate the reliability of our estimated rotational constants.

SUMMARY

The high-resolution absorption spectrum of the $S_1 \leftarrow S_0$ 0_0^0 band of FBPc was observed using the buffer-gas cooling technique and a single-mode tunable laser. In this study, we improved our experimental and analytical methods for better reliability compared to our previous research. The observed spectrum was accurately reproduced through simulation and contour fitting, assuming an a-type transition where the transition moment is parallel to the rotational principal axis $x(a)$. Therefore, we conclude that the transition is a-type, and the S_1 state is $^1B_{3u}$, consistent with Ref. 32. The fitting indicated a rotational temperature of 6 K and a Doppler width of 0.0016 cm^{-1}, corresponding to a translational temperature of 10 K.

The best-fit rotational constants in the S_0 state aligned well with both those in Ref. 32 and the calculated values using MN15/6-31G(d) under the assumption of D_{2h} symmetry. Slightly negative inertial defects in the S_0 and S_1 can be explained by the empirical formula. The larger B in the S_1 state can be understood through the characters of $4a_u$ and $6b_{3g}$ molecular orbitals, which are the main components in the $S_1 \leftarrow S_0$ transition.

ACKNOWLEDGMENTS

We thank Professor Doyle, Professor Takahashi, Professor Hutzler, Professor Uetake, and Professor Takasu for their kind cooperation. Y.M. thanks the members of Core for Quantum Universe (RIIS, Okayama University). This work was supported by JSPS KAKENHI Grant Nos. 18H01229, 21K05105, 22H01249, and 23K03277.

AUTHOR DECLARATIONS

Conflict of Interest

The authors have no conflicts to disclose.

Author Contributions

Yuki Miyamoto: Conceptualization (equal); Data curation (lead); Funding acquisition (lead); Investigation (lead); Methodology (equal); Project administration (lead); Validation (lead); Visualization (lead); Writing – original draft (equal). **Ayami Hiramoto**: Investigation (supporting); Methodology (equal); Writing – review & editing (equal). **Kana Iwakuni**: Conceptualization (equal); Funding acquisition (supporting); Methodology (equal); Writing – review & editing (equal). **Susumu Kuma**: Conceptualization (equal); Funding acquisition (supporting); Methodology (equal); Writing – review & editing (equal). **Katsunari Enomoto**: Conceptualization (equal); Funding acquisition (supporting); Methodology (equal); Writing – review & editing (equal). **Naofumi Nakayama**: Formal analysis (equal); Software (lead); Visualization (supporting); Writing – review & editing (equal). **Masaaki Baba**: Formal analysis (equal); Methodology (equal); Visualization (supporting); Writing – original draft (equal).

DATA AVAILABILITY

The data that support the findings of this study can be obtained from the corresponding author upon reasonable request.

REFERENCES

[1] H. R. Saibil, "Cryo-EM in molecular and cellular biology," Mol. Cell **82**, 274–284 (2022).

[2] K. Bian, C. Gerber, A. J. Heinrich, D. J. Müller *et al.*, "Scanning probe microscopy," Nat. Rev. Methods Primers **1**, 36 (2021).

[3] S. M. Skoff, R. J. Hendricks, C. D. J. Sinclair, M. R. Tarbutt, J. J. Hudson, D. M. Segal, B. E. Sauer, and E. A. Hinds, "Doppler-free laser spectroscopy of buffer-gas-cooled molecular radicals," New J. Phys. **11**, 123026 (2009).

[4] J. Piskorski, D. Patterson, S. Eibenberger, and J. M. Doyle, "Cooling, spectroscopy and non-sticking of *trans*-stilbene and Nile Red," ChemPhysChem **15**, 3800–3804 (2014).

[5] L. Santamaria, V. D. Sarno, I. Ricciardi, M. De Rosa, S. Mosca, G. Santambrogio, P. Maddaloni, and P. De Natale, "Low-temperature spectroscopy of the $^{12}C_2H_2$ ($\nu_1 + \nu_3$) band in a helium buffer gas," Astrophys. J. **801**, 50 (2015).

[6] L. Santamaria, V. D. Sarno, P. D. Natale, M. D. Rosa, M. Inguscio, S. Mosca, I. Ricciardi, D. Calonico, F. Levi, and P. Maddaloni, "Comb-assisted cavity ring-down spectroscopy of a buffer-gas-cooled molecular beam," Phys. Chem. Chem. Phys. **18**, 16715 (2016).

[7] B. Spaun, P. B. Changala, D. Patterson, B. J. Bjork, O. H. Heckl, J. M. Doyle, and J. Ye, "Continuous probing of cold complex molecules with infrared frequency comb spectroscopy," Nature **533**, 517 (2016).

[8] G. Z. Iwata, R. L. McNally, and T. Zelevinsky, "High-resolution optical spectroscopy with a buffer-gas-cooled beam of BaH molecules," Phys. Rev. A **96**, 022509 (2017).

[9] W. Bu, T. Chen, G. Lv, and B. Yan, "Cold collision and high-resolution spectroscopy of buffer-gas-cooled BaF molecules," Phys. Rev. A **95**, 032701 (2017).

[10] S. K. Tokunaga, R. J. Hendricks, M. R. Tarbutt, and B. Darquié, New J. Phys. **19**, 053006 (2017).

[11] V. Di Sarno, R. Aiello, M. De Rosa, I. Ricciardi, S. Mosca, G. Notariale, P. De Natale, L. Santamaria, and P. Maddaloni, "Lamb-dip spectroscopy of buffer-gas-cooled molecules," Optica **6**, 436–441 (2019).

[12] P. B. Changala, M. L. Weichman, K. F. Lee, M. E. Fermann, and J. Ye, "Rovibrational quantum state resolution of the C_{60} fullerene," Science **363**, 49 (2019).

[13] R. Albrecht, M. Scharwaechter, T. Sixt, L. Hofer, and T. Langen, "Buffer-gas cooling, high-resolution spectroscopy, and optical cycling of barium monofluoride molecules," Phys. Rev. A **101**, 013413 (2020).

[14] L. Santamaria, V. Di Sarno, R. Aiello, M. De Rosa, I. Ricciardi, P. De Natale, and P. Maddaloni, "Infrared comb spectroscopy of buffer-gas-cooled molecules: Toward absolute frequency metrology of cold acetylene," Int. J. Mol. Sci. **22**, 250 (2021).

[15] W. Bu, Y. Zhang, Q. Liang, T. Chen, and B. Yan, "Saturated absorption spectroscopy of buffer-gas-cooled barium monofluoride molecules," Front. Phys. **17**, 62502 (2022).

[16] M. Doppelbauer, S. C. Wright, S. Hofsäss, B. G. Sartakov, G. Meijer, and S. Truppe, "Hyperfine-resolved optical spectroscopy of the $A^2\Pi \leftarrow X^2\Sigma^+$ transition in MgF," J. Chem. Phys. **156**, 134301 (2022).

[17] R. Aiello, V. Di Sarno, M. G. Delli Santi, M. De Rosa, I. Ricciardi, P. De Natale, L. Santamaria, G. Giusfredi, and P. Maddaloni, "Absolute frequency metrology of buffer-gas-cooled molecular spectra at 1 kHz accuracy level," Nat. Commun. **13**, 7016 (2022).

[18] G. Z. Zhu, D. Mitra, B. L. Augenbraun *et al.*, "Functionalizing aromatic compounds with optical cycling centres," Nat. Chem. **14**, 995–999 (2022).

[19] Y. Takahashi, M. Baba, K. Enomoto, A. Hiramoto, K. Iwakuni, S. Kuma, R. Tobaru, and Y. Miyamoto, "Low-J transitions in $\tilde{A}^2\Pi(0,0,0)$–$\tilde{X}^2\Sigma^+(0,0,0)$ band of buffer-gas-cooled CaOH," Astrophys. J. **936**, 97 (2022).

[20] K. Enomoto, A. Nakano, T. Suzuki, K. Kobayashi, Y. Takahashi, Y. Miyamoto, and M. Baba, "High-resolution spectroscopy of the $X0^+ \rightarrow A0^+$, $C0^+$ transitions of PbO in 22300–25100 cm^{-1}," J. Mol. Spectrosc. **390**, 111723 (2022).

[21] A. Hiramoto, M. Baba, K. Enomoto, K. Iwakuni, S. Kuma, Y. Takahashi, R. Tobaru, and Y. Miyamoto, "Measurement of Doppler effects in a cryogenic buffer-gas cell," Phys. Rev. A **107**, 043114 (2023).

[22] Y. Miyamoto, R. Tobaru, Y. Takahashi, A. Hiramoto, K. Iwakuni, S. Kuma, K. Enomoto, and M. Baba, "Doppler-free spectroscopy of buffer-gas-cooled calcium monohydroxide," J. Phys. Chem. A **127**, 4758 (2023).

[23] L. Edwards and M. Gouterman, "Porphyrins: XV. Vapor absorption spectra and stability: Phthalocyanines," J. Mol. Spectrosc. **33**, 292–310 (1970).

[24] V. E. Bondybey and J. H. English, "Spectra of the H_2 phthalocyanine in low-temperature matrices," J. Am. Chem. Soc. **101**, 3446–3450 (1979).

[25] P. S. H. Fitch, L. Wharton, and D. H. Levy, "The fluorescence spectrum of free base phthalocyanine cooled in a supersonic free jet," J. Chem. Phys. **70**, 2018 (1979).

[26] P. S. H. Fitch, C. A. Haynam, and D. H. Levy, "The fluorescence excitation spectrum of free base phthalocyanine cooled in a supersonic free jet," J. Chem. Phys. **73**, 1064 (1980).

[27] J. A. Menapace and E. R. Bernstein, "Spectroscopic studies of phthalocyanines and their clusters with small molecules," J. Chem. Phys. **87**, 6877 (1987).

[28] F. L. Plows and A. C. Jones, "Laser-desorption supersonic jet spectroscopy of phthalocyanines," J. Mol. Spectrosc. **194**, 163 (1999).

[29] M. Hartmann, A. Lindinger, J. Peter Toennies, and A. F. Vilesov, "The phonon wings in the ($S_1 \leftarrow S_0$) spectra of tetracene, pentacene, porphin and phthalocyanine in liquid helium droplets," Phys. Chem. Chem. Phys. **4**, 4839–4844 (2002).

[30] R. Lehnig, M. Slipchenko, S. Kuma, T. Momose, B. Sartakov, and A. Vilesov, "Fine structure of the $S_1 \leftarrow S_0$ band origins of phthalocyanine molecules in helium droplets," J. Chem. Phys. **121**, 9396 (2004).

[31] A. Slenczka, "Electronic spectroscopy of phthalocyanine and porphyrin derivatives in superfluid helium nanodroplets," Molecules **22**, 1244 (2017).

[32] F. Schlaghaufer and A. Slenczka, "Electronic spectroscopy of phthalocyanine in a supersonic jet revisited," Phys. Chem. Chem. Phys. **24**, 20921 (2022).

[33] Y. Miyamoto, R. Tobaru, Y. Takahashi, A. Hiramoto, K. Iwakuni, S. Kuma, K. Enomoto, and M. Baba, "High-resolution spectroscopy of buffer-gas-cooled phthalocyanine," Commun. Chem. **5**, 161 (2022).

[34] H. Kato, S. Kasahara, M. Misono, and M. Baba, *Doppler-Free High Resolution Spectral Atlas of Iodine Molecule 15000–19000 cm^{-1}* (Japan Society for the Promotion of Science, Tokyo, 2000).

[35]M. J. Frisch *et al.*, *Gaussian 16, Revision C.01*, Gaussian, Inc., Wallingford, CT, 2016.
[36]C. M. Western, "PGOPHER: A program for simulating rotational, vibrational and electronic spectra," J. Quant. Spectrosc. Radiat. Transfer **186**, 221–242 (2017).
[37]J. K. G. Watson, in *Vibrational Spectra and Structure*, edited by J. R. Durig (Marcel Dekker, New York, 1977), Vol. 6, Chap. 1.
[38]K. Toyota, J. Hasegawa, and H. Nakatsuji, "Excited states of free base phthalocyanine studied by the SAC-CI method," J. Phys. Chem. A **101**, 446 (1997).
[39]R. Fukuda, M. Ehara, and H. Nakatsuji, "Excited states and electronic spectra of extended tetraazaporphyrins," J. Chem. Phys. **133**, 144316 (2010).
[40]J. D. Chai and M. Head-Gordon, "Long-range corrected hybrid density functionals with damped atom–atom dispersion corrections," Phys. Chem. Chem. Phys. **10**, 6615–6620 (2008).
[41]A. Austin, G. A. Petersson, M. J. Frisch, F. J. Dobek, G. Scalmani, and K. Throssell, "A density functional with spherical atom dispersion terms," J. Chem. Theory Comput. **8**, 4989–5007 (2012).
[42]H. S. Yu, X. He, S. L. Li, and D. G. Truhlar, "MN15: A Kohn–Sham global-hybrid exchange–correlation density functional with broad accuracy for multi-reference and single-reference systems and noncovalent interactions," Chem. Sci. **7**, 5032–5051 (2016).
[43]W. M. van Herpen, W. L. Meerts, and A. Dymanus, "Rotationally resolved laser spectroscopy of tetracene and its van der Waals complexes with inert gas atoms," J. Chem. Phys. **87**, 182 (1987).
[44]M. Baba, M. Saitoh, K. Taguma, K. Shinohara, K. Yoshida, Y. Semba, S. Kasahara, N. Nakayama, H. Goto, T. Ishimoto, and U. Nagashima, "Structure and excited-state dynamics of anthracene: Ultrahigh-resolution spectroscopy and theoretical calculation," J. Chem. Phys. **130**, 134315 (2009).
[45]T. Oka, "On negative inertial defect," J. Mol. Struct. **352–353**, 225–233 (1995).